

# Evidence of lower-mantle slab penetration phases in plate motions

Saskia Goes<sup>1</sup>, Fabio A. Capitanio<sup>2†</sup> & Gabriele Morra<sup>2</sup>

It is well accepted that subduction of the cold lithosphere is a crucial component of the Earth's plate tectonic style of mantle convection. But whether and how subducting plates penetrate into the lower mantle is the subject of continuing debate, which has substantial implications for the chemical and thermal evolution of the mantle<sup>1,2</sup>. Here we identify lower-mantle slab penetration events by comparing Cenozoic plate motions at the Earth's main subduction zones<sup>3</sup> with motions predicted by fully dynamic models of the upper-mantle phase of subduction, driven solely by **downgoing plate density**<sup>4</sup>. Whereas subduction of older, intrinsically denser, lithosphere occurs at rates consistent with the model, younger lithosphere (of ages less than about 60 Myr) often subducts up to two times faster, while trench motions are very low. We conclude that the most likely explanation is that older lithosphere, subducting under significant trench retreat, tends to lie down flat above the transition to the high-viscosity lower mantle, whereas younger lithosphere, which is less able to drive trench retreat and deforms more readily, buckles and thickens. Slab thickening enhances buoyancy (volume times density) and thereby Stokes sinking velocity, thus facilitating fast lower-mantle penetration. Such an interpretation is consistent with seismic images of the distribution of subducted material in upper and lower mantle<sup>5,6</sup>. Thus we identify a direct expression of time-dependent flow between the upper and lower mantle.

Seismic methods image anomalies at locations of present and past subduction in upper and lower mantle. These correlate quite well with the history of subduction extending back to 200 Myr ago, if lower-mantle slab sinking rates average about 1–2 cm yr<sup>-1</sup> (refs 7, 8). Only in a few locations do slab anomalies continue directly into the lower mantle, and mostly they do not extend to depths much larger than about 1,500 km (refs 5, 6, 9, 10). Elsewhere, slabs flatten and deform near the base of the upper mantle<sup>5,6,11,12</sup>, and lower-mantle anomalies are unconnected. Seismic methods can only image the current state of the mantle, and do not reveal when material entered the lower mantle, or even whether the lower-mantle anomalies are the result of thermal coupling rather than mass flux<sup>13</sup>.

The one to two orders of magnitude increase in viscosity and endothermic phase change that comprise the transition from upper to lower mantle both hamper flow into the lower mantle. Numerical models have shown that this can lead to time-dependent lower-mantle slab penetration<sup>14–18</sup>, where subduction occurs in several stages. At first, subduction under rapid trench retreat results in pooling of material at the base of the upper mantle<sup>19</sup>. Then, when a sufficiently large mass has accumulated, it sinks into the lower mantle, accompanied by a strong increase in subduction velocity and drop in trench retreat rates<sup>17,18</sup>.

No one has previously looked for such signatures in past plate motions, and, even for the present day, it is debated what governs

the motions<sup>20,21</sup>. It is generally agreed that subduction is driven by downgoing-plate negative buoyancy. Yet most present-day subduction velocities and slab dips display little correlation with plate age, the main control on buoyancy, and other forces have been proposed to play an important part<sup>3,20,21</sup>. Also, it is not understood why most of today's subduction velocities are confined to a range of about 4–9 cm yr<sup>-1</sup>, in spite of a large variation in plate sizes, and regional tectonics<sup>20</sup>.

Using a fully dynamic model (see Supplementary Information and ref. 4), we have characterized plate motions and morphologies during the first subduction phase (when it is confined to the upper mantle) for a freely subducting plate. Free subduction is the most basic form of subduction, driven solely by downgoing plate buoyancy and resisted passively by the mantle and an overriding plate. These models provide a baseline to distinguish phases of upper-mantle-confined subduction from phases where subduction may be penetrating the lower mantle. Most other subduction models are not fully dynamic and impose Earth-like plate or trench motions. But to understand what controls these motions, fully dynamic models—where plate motions and morphology can adjust self-consistently—are required.

The main free subduction characteristics emerging from our models<sup>4</sup> are: (1) slab sinking velocities,  $v_{\text{sink}}$ , are Stokes velocities, that is, they are controlled only by slab density and shape, and by mantle viscosity<sup>4,14</sup>. For realistic effective plate viscosities, two to three orders of magnitude stronger than the upper mantle (see, for example, refs 20, 22), forces that would try to push plates down faster than this will result in slab deformation and thickening, thereby increasing slab Stokes velocity, while forces that try to hold the slab back (for example, resistance to plate bending at the trench), will result in slab detachment or viscous dripping. (2) The plate's strength generally does not allow it to bend to a vertical dip on the timescale it takes to sink into the mantle. As a result, plates with a higher strength, but the same slab buoyancy (that is, same sinking velocity), subduct at a smaller dip, and faster rate,  $v_{\text{sub}}$ . (3) Free subduction occurs basically by trench retreat, at a rate<sup>4,23</sup>  $v_{\text{tr}} = v_{\text{sub}} \cos \alpha_d = v_{\text{sink}} \tan \alpha_d$ , where the dip  $\alpha_d$  is that of the downgoing slab between 100 and 400 km depth, that is, below the bend. Thus, like  $v_{\text{sub}}$ , trench retreat increases with plate density and with plate strength. (4) Plate advance,  $v_{\text{ad}}$ , only occurs to the extent that it is required to preserve continuity between the unsubducted and subducted plate, that is, for a plate that does not stretch or thicken,  $v_{\text{ad}} = v_{\text{sub}} - v_{\text{tr}} = v_{\text{sink}} [1 - \cos \alpha_d] / \sin \alpha_d$ . Thus, the highest possible rate of free plate advance (at  $\alpha_d = 90^\circ$ , and  $v_{\text{tr}} = 0$ ) is the Stokes sinking velocity. Factors that increase the ratio of plate advance over trench retreat are ridge push (the gravitational sliding of plates from the ridge to the trench), a low-viscosity asthenosphere at the base of the plate, and large plate widths<sup>4,24–26</sup>. The few other published dynamic free subduction models display subduction styles similar to ours, where

<sup>1</sup>Department of Earth Science and Engineering, Imperial College London, London SW7 2AZ, UK. <sup>2</sup>Institute of Geophysics, ETH Zurich, 8093 Zurich, Switzerland. <sup>†</sup>Present address: School of Mathematical Sciences, Monash University, Clayton, Victoria 3800, Australia.

conditions are the same<sup>17,18,23,25–27</sup>. Where other models, or natural subduction zones, display behaviour different from these free subduction characteristics, external forces/constraints play a part.

We compare our model velocities with the Cenozoic motions at the world's main subduction zones from the recent update of the global lithospheric age–plate velocity data base of ref. 3. Natural subduction is characterized by low trench retreat, with rates averaging 0.1–0.3 times plate advance rates, throughout the Cenozoic. Furthermore, trench motions are often episodic, and display expressions of outside forcing<sup>21</sup> (Supplementary Information). This explains why a plate-buoyancy signature has only been recognized in present-day absolute plate advance rates (that is, motions of the downgoing plate in a hotspot-reference frame)<sup>28</sup>. Recent data<sup>3,21</sup> confirm the age trend, and it is compatible with an upper-mantle Stokes sinking velocity limit on plate advance, like our models predict for free subduction (Fig. 1). The limiting Stokes velocities for a very reasonable average upper-mantle viscosity of  $(0.5–1.0) \times 10^{21}$  Pa s bracket most of today's slab sinking velocities, as estimated from surface motions and deep dips (Supplementary Fig. 2). An age trend is less apparent in convergence velocities, which are the sum of plate-advance and trench motions, because of the variability of the latter (Supplementary Information).

The range of present-day subduction and plate-advance motions is limited, as in our models (where subduction is driven only by upper-mantle slab buoyancy), with one clear exception. Under Central America, sinking and plate-advance velocities are 40–100% higher than expected for the young age of the plate at the Middle America

trench, which should give it a buoyancy barely negative enough for self-sustained subduction (Fig. 1, Supplementary Information). These high velocities require an enhanced Stokes velocity, implying either a very low-viscosity upper mantle (about an order of magnitude lower than everywhere else, which seems unreasonable), or increased mass as in the case of lower-mantle penetration. This last explanation is compatible with seismic tomography, where the anomaly attributed to subduction under Central America is the only relatively unambiguous example of a continuous slab-like anomaly into the mid to deep lower mantle<sup>6,10</sup>.

The Cenozoic history of motions at the major Pacific and Southeast Asian subduction zones<sup>3</sup> contains more examples of very high plate-advance rates (dips and therefore sinking velocities are not known back in time), all associated with subduction of relatively young lithosphere. And not only the advance velocities, which carry uncertainties associated with the choice of hotspot-reference frame, but also the (reference-frame independent) subduction velocities strongly exceed model rates at these times (Supplementary Fig. 4). The clearest examples of upper-mantle slab-buoyancy driven and faster modes of subduction are shown in Fig. 2.

The Japan-Kurile-Kamchatka and Aleutians-Alaska zones (designated Japan and Alaska hereafter) (Fig. 2a and b) display a clear switch from one mode to another. In both zones, advance velocities for the past 25 Myr lie within the Stokes velocities for upper-mantle confined slabs that fit present-day sinking velocities (Fig. 1). Japan's recent velocities cluster along a single Stokes trend, while Alaska's define a somewhat higher and less tightly clustered age trend. Before 25 Myr ago, there is no age trend and velocities are 1.5–2 times higher than those of similarly aged lithosphere subducted along these trenches today, and 2–3 times higher than the model trend through the recent Japan velocities. Subduction velocities below Middle America have been excessively high for its age throughout most of the past 55 Myr (Fig. 2c). Only between 50 and 55 Myr ago, and for the northern part of the Cocos subduction in the past 10 Myr, do the values approach those of upper-mantle confined slabs. Tonga (Fig. 2d) exhibits the opposite behaviour. Its velocities for the past 45 Myr do not exceed the range for upper-mantle slab buoyancy.

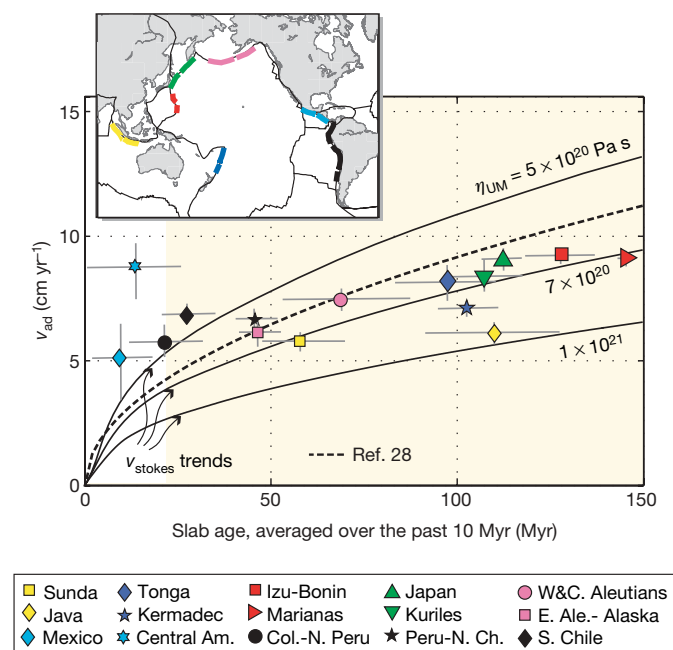


**Figure 1 | Present-day plate-advance velocities.** Main panel, absolute downgoing plate motions,  $v_{ad}$ , versus upper-mantle slab age (plate age at the trench averaged over the last 10 Myr of subduction) from the compilation of ref. 3 compared with Stokes velocities for upper-mantle slabs (1,000 km width and upper-mantle viscosity,  $\eta_{UM}$ , of  $(1.0, 0.7, 0.5) \times 10^{21}$  Pa s (or constant  $\eta_{UM}$  of  $1.0 \times 10^{21}$  Pa s and plate widths of 1,000, 2,000, 3,000 km, respectively). For comparison with the data, model densities were converted to equivalent plate ages using the parameters from ref. 30. For slab ages less than 20 Myr, subduction is probably not self-sustaining (white background). The error bars represent the full range of variation within each trench segment. Trends are similar when slab age is averaged over 5 or 15 Myr. The trend of ref. 28 also fits the recent data presented here. Inset, map of the zone segments used. Segmentation scale corresponds to scale at which the main variations in plate motions and dip occur. Figure key gives names. Abbreviations: Ale., Aleutians; Am., America; Ch., Chile; Col., Columbia; N., North; S., South; E., East; W&C., West and Central.

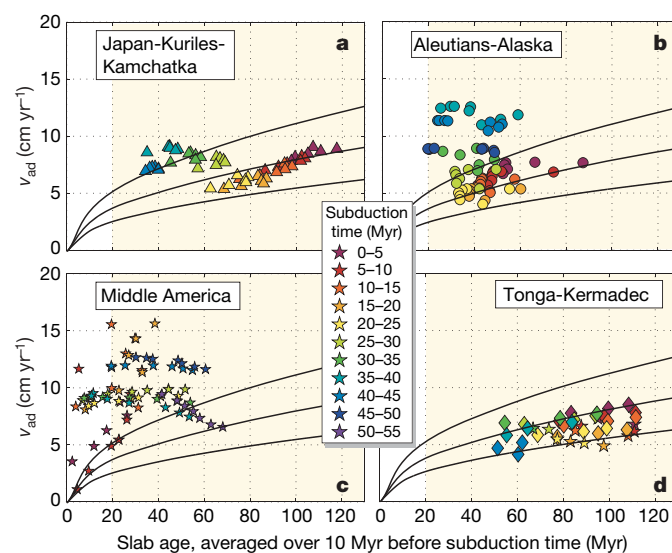


**Figure 2 | Past plate-advance velocities.** a–d, Comparison between Cenozoic advance velocities of the downgoing plate,  $v_{ad}$ , versus average upper-mantle slab age, and the upper-mantle slab Stokes velocities that bracket present-day sinking rates (Fig. 1 main panel; probably only self-sustaining above 20 Myr slab age); data are given for selected zones (Fig. 1 inset) shown boxed in each panel. Velocities are shown at points spaced 500 km along the trench, exactly as in ref. 3, because an appropriate segmentation would vary in time. In d, different symbols are used for the Tonga (diamonds) and Kermadec (stars) sections of the trench.

There is a trend of velocity with age, specifically for Tonga. Subduction at the Kermadec end of the trench has probably been slowed down by subduction of the Louisville ridge and the Hikurangi plateau.

Interestingly, the phases of the highest excess downgoing-plate velocities coincide with minima in trench velocities, both in absolute sense and relative to subduction velocities (Supplementary Fig. 3), similar to the signature that models display during lower-mantle slab penetration<sup>17,18</sup>. Trench motions in Japan and Alaska reach a minimum of 0.07 times plate-advance. Minimum trench/plate motion ratios at the Middle America trench are slightly higher, 0.1–0.2, but absolute and relative retreat velocities are at least a factor of two lower than between 50 and 55 Myr ago. For Tonga, rollback velocities are generally quite high with phases of active back-arc spreading. We interpret these observations as evidence for past lower-mantle penetration in Japan and Alaska, almost continuous Cenozoic lower-mantle penetration under Middle America, and upper-mantle confined subduction below Tonga for the past 45 Myr.

The inferred lower-mantle penetration phases are compatible with seismic tomography. Material sinking into the lower mantle since 50 or 25 Myr ago, at rates of 1–2 cm yr<sup>-1</sup>, would have reached a depth of 1,150–1,650 or 900–1,150 km, respectively. The Farallon anomaly below Middle America and the northern part of South America (where some of today's sinking velocities are also quite high; Fig. 1) is strongest down to about 1,700 km depth<sup>5,6</sup>, compatible with 50 Myr of continuous slab sinking into the lower mantle. Under South America, where relatively young lithosphere subducted throughout the Cenozoic, periods of very high subduction velocities, coincident with minima in trench retreat, also occur, especially at the northern end<sup>3</sup> (Supplementary Fig. 5). The tomographic models also image high-velocity material in the lower mantle below Japan at least down to about 1,000–1,200 km, possibly deeper. In the upper mantle, the Japan and southern Kurile slabs are flattened above the 660 km discontinuity, and the imaged upper-mantle slab length is similar to the 1,500–2,000 km slab subducted in the past 25 Myr. The amount of flattening and the subduction velocities decrease northwards until lower- and upper-mantle anomalies align under Kamchatka<sup>5,6</sup>. Under Alaska and the Aleutians, upper-mantle tomography away from the trench is not well resolved, but a flat slab seems to be present

in the transition zone below the Aleutians<sup>6</sup>, while material down to about 1,300 km depth is found below the eastern Aleutians-Alaska<sup>9</sup>. The imaged Tonga slab also flattens in the transition zone and its length can account for the past 45 Myr of subduction. The same holds for Izu-Bonin, where exceedance of upper-mantle subduction velocity trends during the ~45 Myr history of this zone is marginal, and until recently there has been significant trench retreat with active back-arc spreading<sup>3</sup> (Supplementary Fig. 5), compatible with the long, flat-lying upper-mantle slab anomaly<sup>5,6</sup>.

It may seem surprising that it is the younger, less buoyant, lithosphere that preferentially penetrates quickly into the lower mantle. However, because of its lower buoyancy, freely subducting young lithosphere drives less trench retreat than old lithosphere (Fig. 3). This effect is enhanced if younger lithosphere also has a lower resistance to bending<sup>4</sup>. In addition, zones subducting younger lithosphere seem often unable to initiate back-arc spreading<sup>3,29</sup>, which further hampers trench retreat. Low trench retreat and low slab strength both encourage slab deformation in the transition zone (Fig. 3).

If trench retreat is facilitated—for example, by a small slab width, as in the case of Calabria or South Sandwich—even young lithosphere may avoid fast lower-mantle penetration. In contrast, if outside forces are sufficient to hamper or force the motion of a trench that consumes old plate, they may induce lower-mantle penetration. This could be happening at the Marianas trench (which has pivoted and advanced around a point near its southern end<sup>3</sup>) and Kermadec (where buoyant lithosphere impinges on the partially advancing trench). In both cases, a steeply dipping slab anomaly is seen to penetrate down to 1,000 km depth<sup>5,6</sup>, although plate-advance velocities are not anomalously high, which may indicate that their lower-mantle penetration is not driven by excess slab buoyancy.

Without thickening, slab Stokes velocities decrease in proportion to the upper-lower mantle viscosity increase, resulting in lower-mantle sinking velocities of at most a few mm yr<sup>-1</sup>. For a viscosity increase by a factor of 10, slabs would need to thicken 1.4–4 times to attain the 1–2 cm yr<sup>-1</sup> lower-mantle sinking velocities that reconcile seismic tomography and subduction history. At a subduction rate of 7 cm yr<sup>-1</sup>, vertically sinking slabs can thicken by that much over a timescale of 14–40 Myr. This timescale is similar to the few tens of Myr over which variations in subduction mode occur in the data (Fig. 2).

Throughout the Cenozoic, subduction of young lithosphere commonly satisfied the conditions of low trench retreat and easy transition-zone thickening, which facilitate free and fast lower-mantle penetration, while old lithosphere usually did not. Such penetration speeds up young plate subduction to rates similar to or higher than the rates at which old plate subducts under the influence of upper-mantle slab pull, thus providing a mechanism that buffers plate motion rates.

Received 10 July 2007; accepted 14 January 2008.

1. Van Keken, P. E., Hauri, E. H. & Ballentine, C. J. Mantle mixing: The generation, preservation and destruction of chemical heterogeneity. *Annu. Rev. Earth Planet. Sci.* **30**, 493–525 (2002).
2. McNamara, A. K. & Van Keken, P. E. Cooling of the Earth: A parameterized convection study of whole versus layered models. *Geochim. Geophys. Geosyst.* **1**, doi:10.1029/2000GC000045 (2000).
3. Sdrólías, M. & Müller, R. D. Controls on back-arc basin formation. *Geochim. Geophys. Geosyst.* **7**, doi:10.1029/2005GC001090 (2006).
4. Capitanio, F. A., Morra, G. & Goes, S. Dynamic models of downgoing plate buoyancy driven subduction: Subduction motions and energy dissipation. *Earth Planet. Sci. Lett.* **262**, 284–297 (2007).
5. Bijwaard, H., Spakman, W. & Engdahl, E. R. Closing the gap between regional and global travel time tomography. *J. Geophys. Res.* **103**, 30055–30078 (1998).
6. Fukao, Y., Widiyantoro, S. & Obayashi, M. Stagnant slabs in the upper and lower mantle transition zone. *Rev. Geophys.* **39**, 291–323 (2001).
7. Ricard, Y., Richards, M. A., Lithgow-Bertelloni, C. & Lestunff, Y. Geodynamic model of mantle density heterogeneity. *J. Geophys. Res.* **98**, 21895–21909 (1993).
8. Van der Voo, R., Spakman, W. & Bijwaard, H. Mesozoic subducted slabs under Siberia. *Nature* **397**, 246–249 (1999).

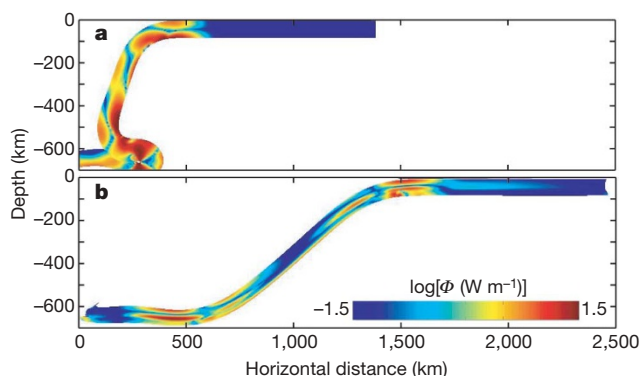


**Figure 3 | Model slab deformation.** Two models (set up as described in Supplementary Information, details in ref. 4) illustrate how deformation above the upper-mantle/lower-mantle boundary depends on plate properties, for plates subjected to ridge push and a low-drag asthenosphere. In **a**, a plate with buoyancy appropriate for a young downgoing slab (equivalent of 49 kg m<sup>-3</sup> density times 80 km thickness), with a uniform viscosity of 100 times that of the surrounding mantle, buckles and thickens. In contrast, in **b**, a plate with old-plate buoyancy (88 kg m<sup>-3</sup> times 80 km), and a strong 17-km-thick core with a viscosity 1,000 times that of the upper mantle (so that average plate viscosity equals 100× upper-mantle viscosity), retreats much more, resulting in a flat lying slab. Both snapshots are after 60% of the plate has been subducted. Colours represent lithospheric energy dissipation ( $\Phi$  = strain rate × stress) at this point in time, where red regions deform strongly and blue regions deform little.

9. Káráson, H. & van der Hilst, R. D. in *The History and Dynamics of Global Plate Motions* (eds Richard, M., Gordon, R. & van der Hilst, R.) 277–288 (American Geophysical Union, Washington DC, 2000).
10. Grand, S., van der Hilst, R. D. & Widiyantoro, S. Global seismic tomography: A snapshot of convection in the Earth. *GSA Today* **7**, 1–7 (1997).
11. Isacks, B. & Molnar, P. Distribution of stresses in the descending lithosphere from a global survey of focal mechanism solutions of mantle earthquakes. *Rev. Geophys.* **9**, 103–174 (1971).
12. Creager, K. C., Chiao, L.-Y., Winchester, J. P. Jr & Engdahl, E. R. Membrane strain rates in the subducting plate beneath South America. *Geophys. Res. Lett.* **22**, 2321–2324 (1995).
13. Cizkova, H., Cadec, O., Van den Berg, A. P. & Vlaar, N. J. Can lower mantle slab-like seismic anomalies be explained by thermal coupling between upper and lower mantles? *Geophys. Res. Lett.* **26**, 1501–1504 (1999).
14. Guillou-Frottier, L., Buttles, J. & Olson, P. Laboratory experiments on the structure of subducted lithosphere. *Earth Planet. Sci. Lett.* **133**, 19–35 (1995).
15. Gurnis, M. & Hager, B. H. Controls of the structure of subducted slabs. *Nature* **335**, 317–321 (1988).
16. Tackley, P. J., Stevenson, D. J., Glatzmaier, G. A. & Schubert, G. Effects of an endothermic phase-transition at 670 km depth in a spherical model of convection in the Earth's mantle. *Nature* **361**, 699–704 (1993).
17. Ita, J. & King, S. D. The influence of thermodynamic formulation on simulations of subduction zone geometry and history. *Geophys. Res. Lett.* **25**, 1463–1466 (1998).
18. Zhong, S. & Gurnis, M. Mantle convection with plates and mobile, faulted plate margins. *Science* **267**, 838–843 (1995).
19. Christensen, U. R. The influence of trench migration on slab penetration into the lower mantle. *Earth Planet. Sci. Lett.* **140**, 27–39 (1996).
20. Conrad, C. P. & Hager, B. H. Effects of plate bending and fault strength at subduction zones on plate dynamics. *J. Geophys. Res.* **104**, 17551–17571 (1999).
21. Lallemand, S., Heuret, A. & Boutelier, D. On the relationships between slab dip, back-arc stress, upper plate absolute motion, and crustal nature in subduction zones. *Geochem. Geophys. Geosyst.* **6**, Q09006, doi:10.1029/2005GC000917 (2005).
22. Moresi, L. & Gurnis, M. Constraints on the lateral strength of slabs from three-dimensional dynamic flow models. *Earth Planet. Sci. Lett.* **138**, 15–28 (1996).
23. Bellahsen, N., Faccenna, C. & Funiciello, F. Dynamics of subduction and plate motion in laboratory experiments: Insights into the “plate tectonics” behavior of the Earth. *J. Geophys. Res.* **110**, 1–15 (2005).
24. Schellart, W. P., Freeman, J., Stegman, D. R., Moresi, L. & May, D. Evolution and diversity of subduction zones controlled by slab width. *Nature* **446**, 308–311 (2007).
25. Stegman, D. R., Freeman, J., Schellart, W. P., Moresi, L. & May, D. Influence of trench width on subduction hinge retreat rates in 3-D models of slab rollback. *Geochem. Geophys. Geosyst.* **7**, Q03012, doi:10.1029/2005GC001056 (2006).
26. Royden, L. H. & Husson, L. Trench motion, slab geometry and viscous stresses in subduction systems. *Geophys. J. Int.* **167**, 881–905 (2006).
27. Enns, A., Becker, T. W. & Schmeling, H. The dynamics of subduction and trench migration for viscosity stratification. *Geophys. J. Int.* **160**, 761–769 (2005).
28. Carlson, R. L., Hilde, T. W. C. & Uyeda, S. The driving mechanism of plate tectonics: Relation to age of the lithosphere at trenches. *Geophys. Res. Lett.* **10**, 297–300 (1983).
29. Molnar, P. & Atwater, T. Interarc spreading and Cordilleran tectonics as alternates related to the age of subducted oceanic lithosphere. *Earth Planet. Sci. Lett.* **41**, 330–340 (1978).
30. Cloos, M. Lithospheric buoyancy and collisional orogenesis: Subduction of oceanic plateaus, continental margins, island arcs, spreading ridges, and seamounts. *Geol. Soc. Am. Bull.* **105**, 715–737 (1993).

**Supplementary Information** is linked to the online version of the paper at [www.nature.com/nature](http://www.nature.com/nature).

**Acknowledgements** We thank M. Sdrolias and D. Müller for sending us their data, and S. King for comments. This work was supported by a Schweizerischer Nationalfonds Förderungsprofessur (to S.G.).

**Author Contributions** The three authors contributed equally to this work.

**Author Information** Reprints and permissions information is available at [www.nature.com/reprints](http://www.nature.com/reprints). Correspondence and requests for materials should be addressed to S.G. (s.goes@imperial.ac.uk).